Research Square

Preprints are preliminary reports that have not undergone peer review.
They should not be considered conclusive, used to inform clinical practice,
or referenced by the media as validated information.

# A Black-Hole-Matter Hypothesis for Spacetime Geometry, Energy and Particles: The Börekci-2 Node-Spacing Metric, Literature Basis and Experimental Constraints

**Hasan Börekci**

hborekci@hotmail.com.tr

HB ZECHMANN Medical Company

**Research Article**

**Keywords:** Börekci hypothesis, quantum vacuum, QCD vacuum, emergent spacetime, black-hole interior, Börekci-2 metric, equivalence principle

**Posted Date:** September 25th, 2026

**DOI:** https://doi.org/10.21203/rs.3.rs-11146762/v1

**License:** This work is licensed under a Creative Commons Attribution 4.0 International License.
Read Full License

**Additional Declarations:** No competing interests reported.

# A Black-Hole-Matter Hypothesis for Spacetime Geometry, Energy and Particles: The Börekci-2 Node-Spacing Metric, Literature Basis and Experimental Constraints

Regular Article

**Hasan Börekci[1]***

[1] Assistant Professor of General Surgery; R&D Director, HB ZECHMANN Medical Company, Manisa Technopark, Celal Bayar University Campus Area, Manisa, Turkey; Independent Theoretical Physics Researcher

* Correspondence: hborekci@hotmail.com.tr · ORCID: https://orcid.org/0000-0001-9137-6342

Version 2.5 · 24 September 2026

---

**Abstract.** A conceptual hypothesis (Börekci's Hypothesis of Black-Hole Matter as the Primary Substance of the Universe) is presented that defines spacetime geometry as "a structure made of black-hole matter joined by special links, mobile and changing according to the gravity and energy within it", and proposes this matter as the primary substance of all spacetime-fabric geometry, energy, atoms and subatomic particles. Four propositions are stated: empty space is the most dilute and the black-hole interior the densest state of this matter (P1); the nodes of the network linking spacetime are made of it (P2); a black hole's gravity arises from the mass it has swallowed (P3); everything swallowed becomes black-hole matter (P4). The literature basis is compiled: experiments showing that the quantum vacuum is not empty (notably the 2026 STAR virtual-quark-pair spin correlation), emergent-spacetime theories, models relating black-hole interiors to the vacuum, the black-hole–particle continuity, and work connecting black holes to the origin of the universe. A node-spacing relation is derived from a constant-proper-spacing postulate, the curvature around the Sun, Earth and Moon is computed with five measures, and a node-spacing metric (the Börekci-2 metric) is defined; it is identical to the Schwarzschild geometry outside the horizon, reproduces GPS and S2-star time dilation, and yields natural markers for the horizon, the photon sphere, the ISCO and the black-hole-matter surface. Because node compression affects all local scales together, the equivalence principle is preserved and atomic-clock constraints are satisfied. Two distinguishing predictions are given: a transition region at the horizon, and a blue tilt of the primordial gravitational-wave spectrum from an early stiff-fluid era. The hypothesis is consistent with, but not proven by, the literature; the steps for a full test are stated.

**Keywords:** Börekci hypothesis; quantum vacuum; QCD vacuum; emergent spacetime; black-hole interior; Börekci-2 metric; equivalence principle

## 1. Introduction

In classical physics, empty space is a region containing nothing. Quantum field theory changed this picture: the vacuum, the lowest-energy state, is a structured medium of continuously fluctuating fields and of quark–antiquark and gluon condensates, and this structure can be measured directly [1, 2]. General relativity describes spacetime as a dynamical geometry that bends in response to matter and energy. What lies beneath this geometry remains one of the open questions of theoretical physics.

The hypothesis proposed here approaches this question through black holes. Seen from outside, all matter that falls into a black hole is reduced to mass, charge and angular momentum (the no-hair theorem) [3]. The hypothesis proposes that behind this reduction, matter is converted into a single ancestral state, "black-hole matter", and that the dilute state of the same matter forms the fabric of spacetime. In the water analogy: the black hole is the densest state of water, and the spacetime fabric is the vapour that fills everything. The original claim of the hypothesis is that matter, energy and spacetime geometry descend from one common ancestor.

The aims of the paper are fourfold: (i) to ground the phenomena on which the hypothesis relies in the literature; (ii) to turn the hypothesis into a quantitative network model and to illustrate it with concrete calculations at Solar-System scale; (iii) to define a metric (the Börekci-2 node-spacing metric) from the network model and to compute the time dilation of bodies with it; (iv) to compare the model's predictions with current experimental data. This hypothesis: Börekci's Hypothesis of Black-Hole Matter as the Primary Substance of the Universe. Established knowledge and proposed interpretation are kept explicitly apart throughout. Section 2 gives the experimental and Section 3 the theoretical background; Section 4 states the hypothesis, Section 5 the quantitative model, the metric and the calculations, Section 6 the predictions and constraints, Section 7 the discussion and Section 8 the conclusions.

## 2. Experimental background: the quantum vacuum is not empty

### *2.1 Zero-point energy and the Casimir force*

In quantum mechanics every field mode carries non-zero energy even in its lowest-energy state:

$$E_0 = \Sigma_k \, \hbar\omega_k / 2 \qquad (1)$$

Casimir [4] calculated that restricting the vacuum modes between two parallel conducting plates produces a force pulling the plates together:

$$F / A = - \pi^2 \hbar \, c / (240 \, d^4) \qquad (2)$$

where d is the plate separation; for d = 1 μm the pressure is about 1.3 mPa. The force was measured in a sphere–plate geometry [5] and with parallel metallic plates [6].

### *2.2 The Lamb shift*

According to Dirac theory the 2S1/2 and 2P1/2 levels of hydrogen should coincide. Lamb and Retherford [7] measured a splitting of about 1057 MHz; Bethe [8] explained most of it through the interaction of the electron with vacuum fluctuations.

### *2.3 Direct measurement of vacuum fluctuations*

Riek et al. [1] directly detected the electromagnetic vacuum fluctuations of free space by electro-optic sampling with few-femtosecond laser pulses; the measured electric-field variance was inversely proportional to the sampled four-dimensional spacetime volume. Benea-

Chelmus et al. [9] measured correlations of the electric field between different spacetime points in the vacuum state.

### *2.4 Real particles from the vacuum*

Wilson et al. [10] produced photon pairs from the vacuum with an effective mirror moved electrically in a superconducting circuit (the dynamical Casimir effect). Schwinger [11] predicted that a sufficiently strong electric field would tear electron–positron pairs from the vacuum; the threshold field is

$$E_S = m_e^2 c^3 / (e \hbar) \approx 1.3 \times 10^{18} \text{ V/m} \qquad (3)$$

This threshold has not yet been reached in the laboratory, but the direct conversion of light into matter has been observed: the STAR Collaboration [12] confirmed the Breit–Wheeler process by measuring 6085 electron–positron pairs from photon–photon collisions, and the ATLAS Collaboration [13] reported evidence for light-by-light scattering.

### *2.5 Virtual quarks in empty space: the QCD vacuum*

In quantum chromodynamics (QCD) the vacuum contains quark–antiquark and gluon condensates [14]. Lattice QCD has shown that the masses of light hadrons can be computed from first principles from quark and gluon dynamics [15]; only a few per cent of the proton mass comes from the quark masses themselves. The proton contains a "sea" of continuously created and annihilated quark–antiquark pairs; the SeaQuest Collaboration [16] found that anti-down quarks outnumber anti-up quarks in this sea.

The most direct finding for the hypothesis is the study published by the STAR Collaboration in Nature in 2026 [2]. High-energy proton–proton collisions can liberate virtual quark–antiquark pairs from the QCD vacuum and turn them into real particles. STAR detected a relative polarization signal of (18 ± 4)% in Λ–anti-Λ hyperon pairs, inherited from spin-correlated virtual strange quark–antiquark pairs; the correlation vanishes when the hyperons are widely separated in angle. This is an experimental indication that virtual quark pairs exist in the QCD vacuum—what we call empty space—and can become real particles. The hypothesis interprets this production as an activity of the black-hole matter that constitutes the structure of spacetime; the scope of this interpretation is fixed in Section 6.2.

> **Note.** Free quarks have never been observed in isolation (colour confinement); the presence of quark pairs in the vacuum is inferred indirectly from the properties of hadrons. The phrase "particles that appear and disappear" is a heuristic; what experiments measure are field fluctuations and correlations.

## 3. Theoretical background

### *3.1 Spacetime emerging from a more fundamental structure*

- Sakharov [17]: gravity arises from the response of quantum vacuum fields to curvature (induced gravity).

- Jacobson [18]: the Einstein equations can be derived from thermodynamics applied to local horizons; they behave like an equation of state.
- Volovik [19]: low-energy excitations of superfluid helium-3 behave like an effective spacetime metric.
- Barceló, Liberati and Visser [20]: analogue gravity; waves in fluids propagate like fields in curved spacetime.
- Rovelli and Smolin [21]: in loop quantum gravity space is described by spin networks whose nodes carry quanta of volume and whose links carry quanta of area; the framework closest to P2.
- Konopka, Markopoulou and Severini [22]: quantum graphity; spacetime emerges through a phase transition of a graph; the model closest to the water–vapour analogy.
- Van Raamsdonk [23] and Verlinde [24]: spacetime connectivity is derived from entanglement, and gravity as an entropic force.

All of these approaches propose a structure beneath spacetime, but none relates it to black holes.

### *3.2 Black holes and the vacuum*

- Hawking [25, 26]: near the horizon vacuum fluctuations become real particles; the black hole emits thermal radiation. Thermal Hawking radiation has been observed in an analogue black hole [27].
- Gravastar [28]: the interior is a vacuum condensate of negative pressure. Fuzzball [29]: a structured surface carrying the black hole's information replaces the sharp horizon. Planck star [30]: collapsing matter is halted at Planck density by quantum-gravitational pressure.
- Wheeler [31] proposed spacetime foam at the Planck scale and Hawking [32] virtual black holes within it. Mäkelä [33] suggested that Planck-size quantum black holes could act as the fundamental constituents of space and time.
- Mathur's vecro hypothesis [34, 35, 36, 37]: the vacuum wavefunctional of quantum gravity contains a component made of virtual fluctuations of black-hole microstates (fuzzballs). These structures exist at all scales; when collapsing matter approaches its horizon they are compressed into real fuzzballs, and in an expanding universe they are stretched and generate vacuum energy. Brandenberger and Mitchell [38] argued that a gas of vecros behaves as a stiff fluid ($p = \rho c^2$) and can halt the collapse of a contracting universe.

The vecro hypothesis is the approach closest to the present one: it holds that empty space contains virtual black-hole structures and that real black holes are their compressed state. The present hypothesis interprets empty space not as virtual fluctuations but as a real, dilute state of black-hole matter.

### *3.3 Black holes and the origin of the universe*

The "ancestor" claim requires black-hole matter to have existed at the beginning of the universe. This idea has counterparts in the literature. Pathria [39] proposed that the universe may be the interior of a black hole. Smolin [40], in cosmological natural selection, argued that a new universe is born inside every black hole, so that universes descend from black holes. Popławski [41] showed that our universe may have formed by a bounce inside a black hole in a larger universe. Banks and Fischler [42] modelled the early universe in holographic cosmology as a dense gas of black holes with pressure equal to energy density ($p = \rho c^2$). In the Planck-star model collapsing matter bounces at Planck density; the black hole and the Big Bang may be two faces of the same physics [30].

### *3.4 The continuity between black holes and elementary particles*

A line of literature that directly supports the "primary matter" claim holds that black holes and elementary particles lie on a continuum. Hawking [43] showed that black holes of very low mass could form in the early universe. 't Hooft [44] argued that black holes are as fundamental as strings and that the two descriptions are complementary. Holzhey and Wilczek [45], in "Black holes as elementary particles", showed that certain black-hole solutions behave like particles. Horowitz and Polchinski [46] established a correspondence principle between black holes and string states: as the mass decreases to the string scale, a black hole passes continuously into a highly excited string state. Dvali and Gomez [47] modelled the black hole as a Bose–Einstein condensate of gravitons at the critical point. These works show that the black hole is a fundamental object standing at the boundary between matter and geometry, and that it may occupy one end of the same continuum as particles. P1 and P4 propose to explain this continuity with a single primary matter: particles are its most dilute, black holes its densest state.

## 4. The hypothesis

### *4.1 The black-hole interior: what is known and what is assumed*

General relativity describes the exterior of the event horizon by a vacuum solution, and this has been confirmed by observation: the gravitational redshift and Schwarzschild precession of the star S2 around Sgr A* [48, 49], the Event Horizon Telescope shadows [50, 51] and gravitational-wave ringdowns [52]. The interior of the horizon is unobservable in principle. Penrose's singularity theorem [53] states that under general relativity and ordinary energy conditions collapse does not stop once a horizon has formed; the predicted singularity, however, is generally regarded as the limit of validity of the theory. Hence the statement "a black hole is a hole in spacetime with no matter inside" is not an observation but the extrapolation of a theory beyond its own limit.

> **Definition.** In this paper "black-hole matter" denotes the state of matter that replaces the singularity under the assumption that quantum-gravitational effects halt the collapse. This assumption is shared with the Planck-star [30] and fuzzball [29] models; the hypothesis openly acknowledges

> that it borrows the collapse-halting mechanism. The Börekci-2 metric of Sections 5.1a and 5.3 gives the natural location of the black-hole-matter surface.

### *4.2 Name of the hypothesis, propositions and one-sentence statement*

> **Name of the hypothesis.** This hypothesis: **Börekci's Hypothesis of Black-Hole Matter as the Primary Substance of the Universe**. In full: the "Hypothesis of Black-Hole Primary Matter as the Primary Substance of All Spacetime-Fabric Geometry, Energy, Atoms and Subatomic Particles in the Universe". The name states the scope of the claim: black-hole matter is the primary substance not only of the spacetime fabric but of all matter and energy in the universe. In the remainder of the text it is referred to as "the hypothesis" or "the Börekci hypothesis".

**P1.** The primary substance of the spacetime fabric is black-hole matter. Empty space is its most dilute state; the black-hole interior is its densest state.

**P2.** The nodes of the network that links regions of spacetime are made of black-hole matter. The links are long in empty space and shortest inside a black hole.

**P3.** The gravitational pull of a black hole arises not from the density of the matter inside it but from the total mass of the matter it has swallowed.

**P4.** All atoms, energy and matter swallowed by a black hole are ultimately converted into black-hole matter.

> **One-sentence statement of the hypothesis.** Spacetime geometry is a structure made of black-hole matter joined by special links; it is mobile and changes according to the gravity and energy within it. Here "changes" refers to the geometry; local physical constants do not change (Section 6.2). This sentence is a definition, not an inference: it fixes what the hypothesis claims and offers no proof. The behaviour of the links is made quantitative in Eq. (4), and the way the structure changes with gravity in Sections 5.2 and 5.3.

### *4.3 Ancestral matter and cosmic chronology*

The elements come from the quark–gluon plasma, which comes from the Big Bang; astrophysical black holes formed after the stars. For black-hole matter to be the ancestor of everything it must already have existed at the beginning. Together with the work of Section 3.3 the hypothesis takes the following form: the universe began from a black-hole-matter state; the quark–gluon plasma is the first intermediate state through which this matter passes as it dilutes; hadrons, nuclei and the elements formed in stars follow; stellar and supermassive black holes return matter to the primary state in accordance with P4 (Fig. 1). The dilute state, the spacetime fabric, is present at every stage of this cycle, and the virtual-particle production of Section 2 is interpreted as the activity of this fabric.

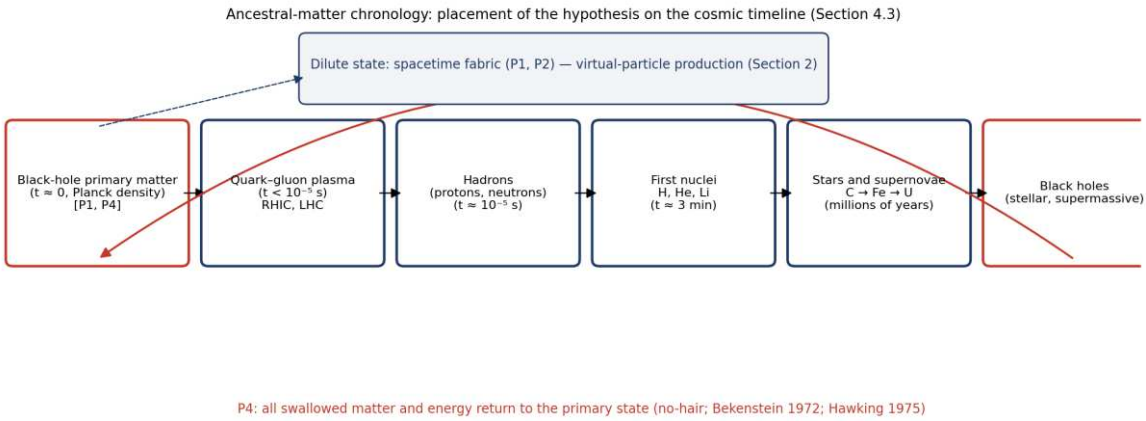



Fig. 1. Primary-matter chronology. The black-hole-matter state is placed at the beginning of the universe; the quark–gluon plasma, hadrons, first nuclei and stellar elements are stages in its dilution. Black holes return swallowed matter to the primary state (P4). The upper box shows the dilute state (the spacetime fabric) present at every stage of the cycle.

## 5. Quantitative model, the Börekci-2 metric and calculations

### *5.1 Network model and node spacing*

As the quantitative form of P2 it is assumed that the spacing between nodes shortens with the local gravitational potential, the fractional shortening being equal to the fractional curvature of spacetime:

$$\ell(r) = \ell_0 \, (1 - |\Phi| / c^2) = \ell_0 \, (1 - r_s / (2r)), \qquad \ell_0 \approx \ell_P = 1.616 \times 10^{-35} \text{ m} \qquad (4)$$

The basic spacing $\ell_0$ in empty space must be of Planck scale, because photons from gamma-ray bursts show no dispersion over billions of light-years. According to Eq. (4) the nodes are sparsest far away and most compressed, at $\ell_0/2$, at the event horizon ($r = r_s$); this value is the same for every black hole. Fig. 2 shows the network in three-dimensional perspective and from three orthogonal directions; Fig. 3 shows the spatial distribution of node spacing as a surface.

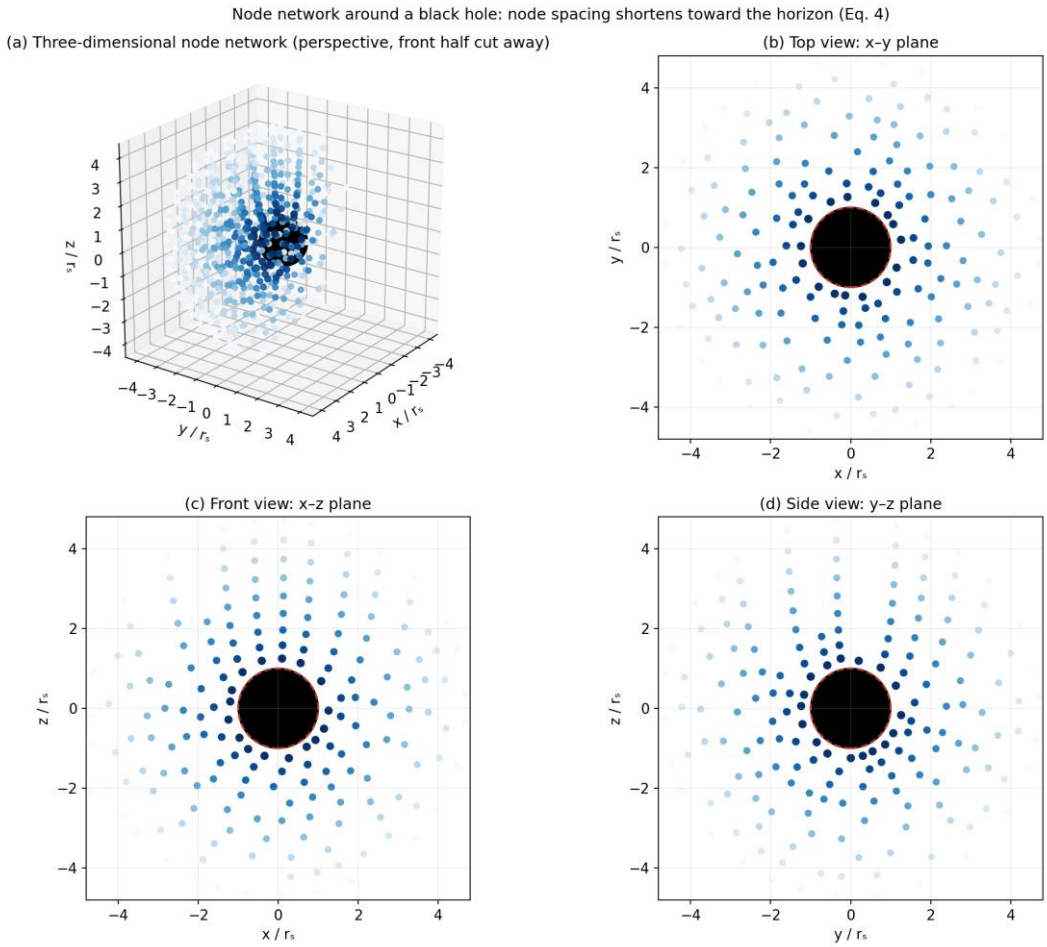



Fig. 2. Node network around a black hole. (a) Three-dimensional perspective; the front half is cut away to reveal the central black hole. (b) Top (x–y), (c) front (x–z) and (d) side (y–z) views, each a thin slice perpendicular to the respective axis. Colour and point size indicate node compression; the black sphere is the event horizon ($r = r_s$). Node spacing from Eq. (4).

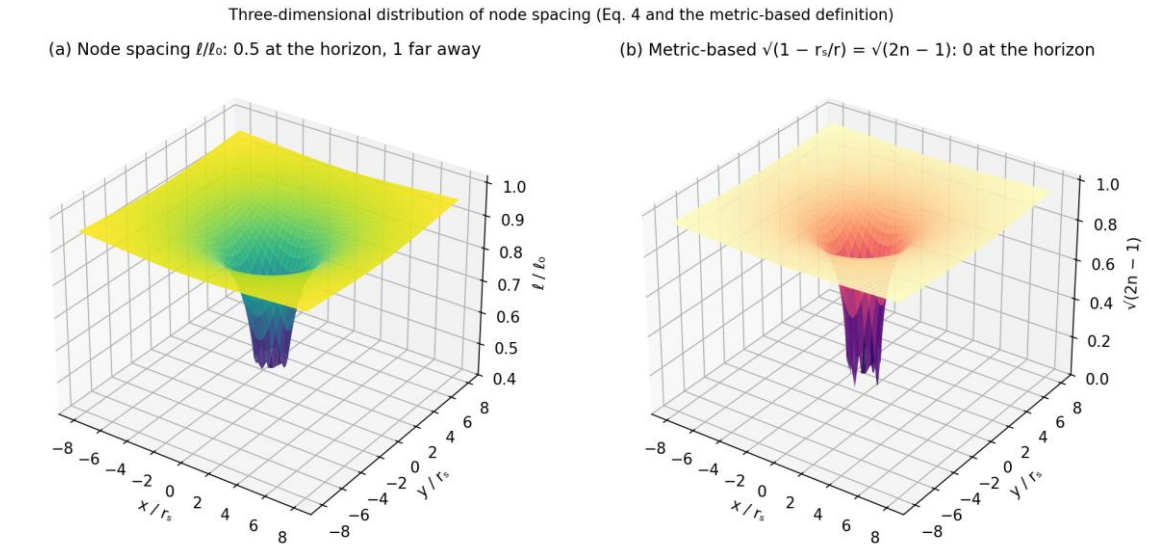



Fig. 3. Three-dimensional distribution of node spacing. (a) Eq. (4): $\ell/\ell_0$ is 0.5 at the horizon and approaches 1 far away. (b) Metric-based definition $\sqrt{(1 - r_s/r)} = \sqrt{(2n - 1)}$: zero at the horizon. The two agree far away and diverge near the horizon; Section 5.3 establishes their relation.

### *5.1a Derivation of Eq. (4): the constant-proper-spacing postulate*

Eq. (4) was presented as an assumption; it can be derived from a single postulate. **Postulate:** the nodes of the network are identical, and the proper length of the link between neighbouring nodes is the same everywhere, $\ell_0 \approx \ell_P$. Outside a spherical body of mass M, in the static spherically symmetric geometry measured with the areal radius r, the radial proper-length element is

$$dl = dr / \sqrt{(1 - r_s / r)} \qquad (4a)$$

so that $dl/\ell_0$ nodes fit into the coordinate interval dr; the node spacing measured in coordinate units is therefore

$$\ell_{coord}(r) = \ell_0 \sqrt{(1 - r_s / r)} \equiv \ell_0 \, n_e(r) \qquad (4b)$$

In the weak field $\sqrt{(1 - r_s/r)} \approx 1 - r_s/(2r) = 1 - |\Phi|/c^2$, so Eq. (4) is the first-order expansion of this exact expression. The exact and linear forms are related exactly by

$$n_e^2 = 1 - r_s / r = 2n - 1 \qquad (4c)$$

This derivation yields three things. (i) The coefficient $2n - 1$ of the metric in Section 5.3 equals $n_e^2$, the square of the coordinate node spacing; the clock rate of a static body equals the coordinate node spacing directly ($d\tau/dt = n_e$). (ii) The two definitions of Fig. 3 are the exact (3b) and approximate (3a) forms of the same quantity; the uncertainty previously flagged as a "caveat" disappears. (iii) In the exact form $n_e$ vanishes at the event horizon ($r = r_s$): the nodes touch at the horizon, and inside it ($n_e^2 < 0$) the network is not defined. The surface of black-hole matter is thus located exactly at the event horizon, the same conclusion as in the fuzzball proposal [29]. The radius $r = GM/c^2 = r_s/2$ at which the linear n vanishes is the point reached by extending the weak-field expansion beyond the horizon; the region between the horizon and this radius ($\Delta r/r_s = 1/2$) is the linear counterpart of the transition region that the exact form compresses into a surface at the horizon.

> **Limit of the derivation.** Together with the postulate, the radial proper-length element of the Schwarzschild geometry has been used; the derivation therefore demonstrates the consistency between the network definition and general relativity, but does not generate the Einstein equations from the network. Obtaining Eq. (4b) from a dynamical principle such as a link energy remains an open item in Section 7.

### *5.2 Spacetime curvature around the Sun, Earth and Moon*

To make the phrase "a structure changing with gravity" concrete, the curvature around the Sun, Earth and Moon is computed with five measures and applied to Eq. (4). Outside a spherical body of mass M the Newtonian potential and the weak-field results of general relativity are [54]:

$$\Phi(r) = - G M / r \qquad (5)$$

$$d\tau / dt = \sqrt{(1 - r_s / r)} \approx 1 - |\Phi| / c^2 \qquad \text{(gravitational time dilation)} \qquad (6)$$

$$\delta = 4\,G\,M / (c^2\,b) \qquad \text{(deflection of light passing at distance b)} \qquad (7)$$

$$K = 48\,G^2\,M^2 / (c^4\,r^6) \qquad \text{(Kretschmann curvature invariant)} \qquad (8)$$

$$a_g = 2\,G\,M\,d / r^3 \qquad \text{(tidal acceleration across a body of length d)} \qquad (9)$$

$$z(r) = 2\,\sqrt{(\,r_s\,(r - r_s)\,)} \qquad \text{(Flamm embedding surface)} \qquad (10)$$

Eq. (6) is the effect corrected daily in GPS satellite clocks [55]; Eq. (7) gives the 1.75 arcseconds measured for the Sun at the 1919 eclipse [56]; Eq. (10) is the embedding of the equatorial plane of the Schwarzschild geometry in three-dimensional Euclidean space [57]. Table 1 gives the surface values.

**Table 1. Measures of spacetime curvature at the surfaces of the Sun, Earth and Moon (Eqs. 5–10) and the node-spacing shortening from Eq. (4).**

| Quantity (at surface) | Sun | Earth | Moon |
|---|---|---|---|
| Mass M (kg) | $1.989 \times 10^{30}$ | $5.972 \times 10^{24}$ | $7.342 \times 10^{22}$ |
| Radius R (m) | $6.957 \times 10^{8}$ | $6.371 \times 10^{6}$ | $1.737 \times 10^{6}$ |
| Schwarzschild radius $r_s$ | 2.95 km | 8.87 mm | 0.109 mm |
| Curvature depth $\lvert\Phi\rvert/c^2$ | $2.12 \times 10^{-6}$ | $6.96 \times 10^{-10}$ | $3.14 \times 10^{-11}$ |
| Clock retardation (per year) | 67 s | 22 ms | 1.0 ms |
| Light deflection, grazing (″) | 1.75 | $5.7 \times 10^{-4}$ | $2.6 \times 10^{-5}$ |
| Kretschmann K ($m^{-4}$) | $9.2 \times 10^{-46}$ | $1.4 \times 10^{-44}$ | $5.2 \times 10^{-45}$ |
| Tidal gradient $2GM/R^3$ ($s^{-2}$) | $7.9 \times 10^{-7}$ | $3.1 \times 10^{-6}$ | $1.9 \times 10^{-6}$ |
| Embedding depth z(R)/R | $4.1 \times 10^{-3}$ | $7.5 \times 10^{-5}$ | $1.6 \times 10^{-5}$ |
| Node shortening, Eq. (4) | $3.4 \times 10^{-41}$ m | $1.1 \times 10^{-44}$ m | $5.1 \times 10^{-46}$ m |

The result is twofold and instructive for the hypothesis. **Curvature depth** ($|\Phi|/c^2$, time dilation, light deflection, embedding depth) is about 68 000 times larger beside the Sun than beside the Moon; by Eq. (4) the nodes beside the Sun are compressed 68 000 times more. **Local curvature** (the Kretschmann invariant and the tidal gradient) scales as $M^2/R^6$ and is therefore larger for dense bodies: the curvature at the Moon's surface is 5.6 times, and at the Earth's surface 15 times, that at the Sun's surface. The same distinction appears at the Earth's location (Table 2): the Sun's potential depth is 70 000 times the Moon's, but the Moon's tidal effect is 2.2 times the Sun's, which is why ocean tides follow the Moon. Figs. 4 and 5 visualise the two measures; Fig. 6 shows the five measures relative to the Sun, and Fig. 7 a three-dimensional landscape of curvature depth in the Earth–Moon system.

**Table 2. Curvature at the Earth's location due to the Sun and the Moon: the Sun dominates in depth, the Moon in local curvature.**

| At the Earth's location | Sun (r = 1 AU) | Moon (r = 384 400 km) |
|---|---|---|
| Curvature depth $\lvert\Phi\rvert/c^2$ | $9.9 \times 10^{-9}$ | $1.4 \times 10^{-13}$ |
| Tidal gradient $2GM/r^3$ ($s^{-2}$) | $7.9 \times 10^{-14}$ | $1.7 \times 10^{-13}$ |
| Node shortening, Eq. (4) | $1.6 \times 10^{-43}$ m | $2.3 \times 10^{-48}$ m |

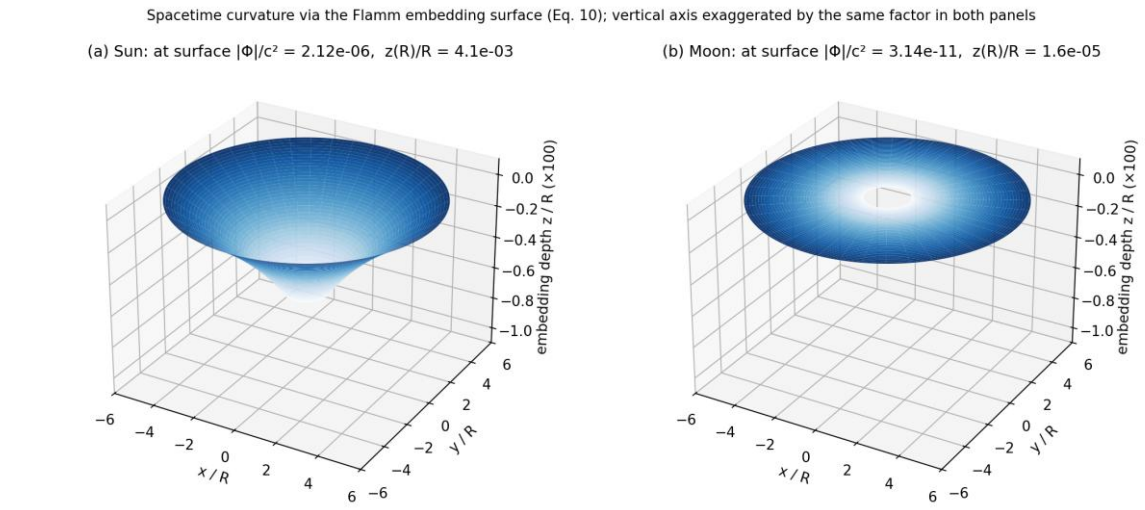



Fig. 4. Flamm embedding surfaces (Eq. 10) for the Sun (a) and the Moon (b), normalised to the radius R, with the vertical axis exaggerated by the same factor (×100) in both panels. The well around the Sun is about 260 times deeper than that around the Moon; without exaggeration both surfaces would look like flat discs.

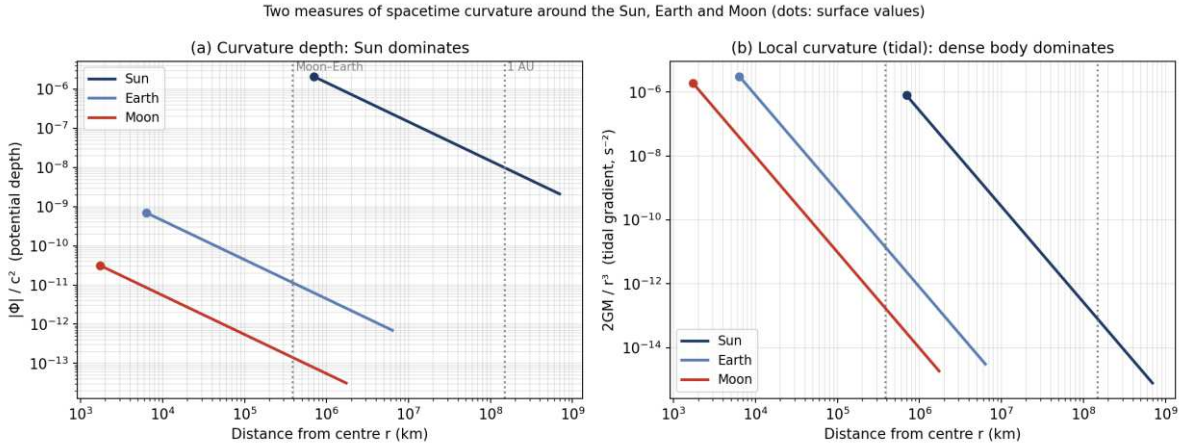



Fig. 5. (a) Curvature depth $|\Phi|/c^2$ and (b) tidal gradient $2GM/r^3$ as functions of distance around the Sun, Earth and Moon. Dots are surface values; vertical lines mark the Moon–Earth distance and 1 AU. The Sun dominates in depth at every distance; the dense body dominates in local curvature near its surface.

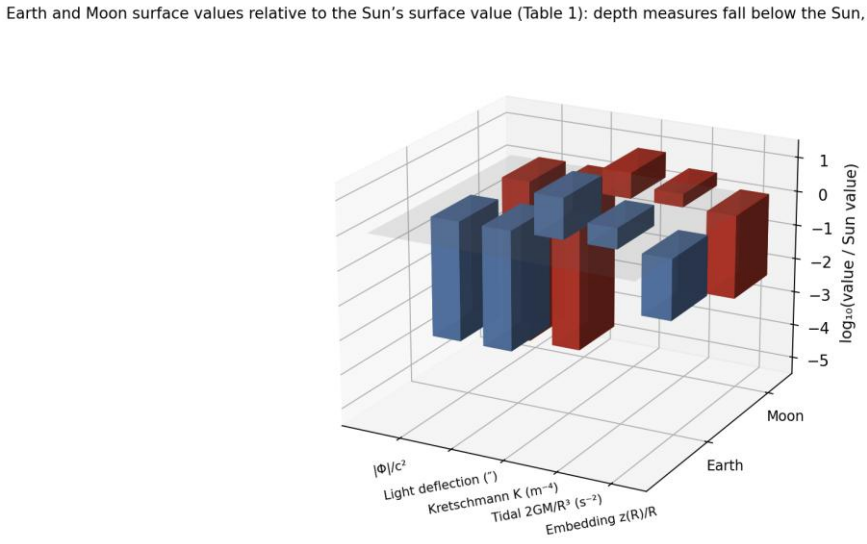



Fig. 6. Earth and Moon surface values of the five curvature measures of Table 1 relative to the Sun's surface value (logarithmic). Depth measures ($|\Phi|/c^2$, light deflection, embedding depth) fall below the Sun; local-curvature measures (Kretschmann invariant, tidal gradient) rise above it.

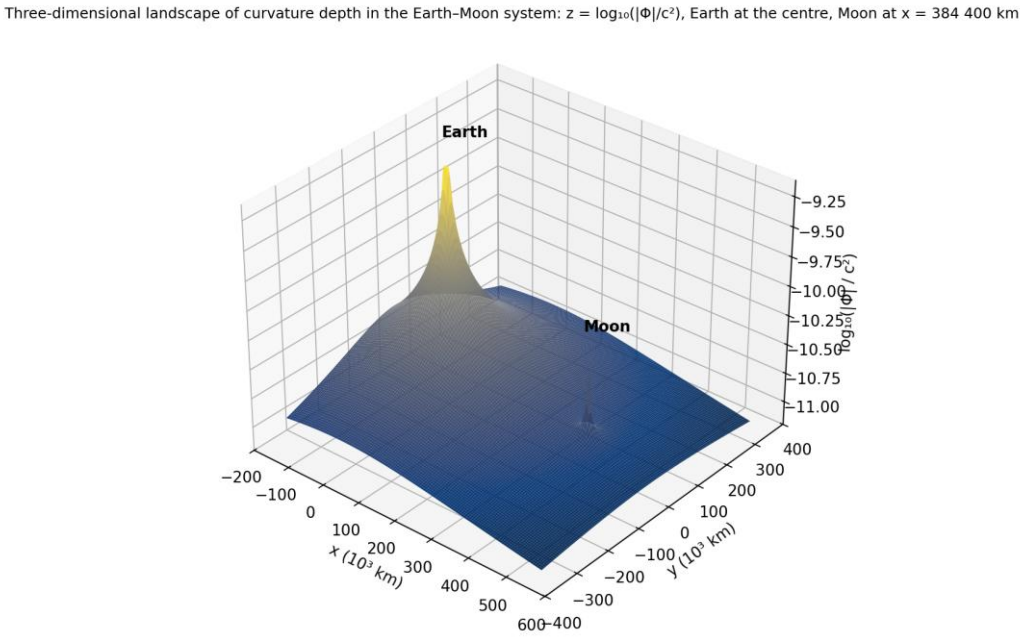



Fig. 7. Three-dimensional landscape of curvature depth in the Earth–Moon system: vertical axis $\log_{10}(|\Phi|/c^2)$, Earth at the centre, Moon at x = 384 400 km. The well around the Earth is far deeper than that around the Moon; the Moon appears as a small well on top of the background Earth potential.

> **Implication for the model.** Eq. (4) ties node spacing to curvature depth; the fabric around the Sun is therefore far more compressed than around the Moon. Local curvature corresponds to the spatial rate of change of node spacing ($d\ell/dr$). "Curvature" in the hypothesis means depth.

### *5.3 The Börekci-2 metric (node-spacing metric)*

To apply the network model to the motion of bodies and to time measurement a metric is required. Taking the node-spacing function $n(r) \equiv \ell(r)/\ell_0 = 1 - GM/(rc^2)$, the following line element is defined for the static, spherically symmetric case and named the **Börekci-2 metric** (node-spacing metric):

$$ds^2 = -(2n - 1)\, c^2\, dt^2 + dr^2 / (2n - 1) + r^2\, d\Omega^2 \qquad (11)$$

$$n(r) = 1 - GM / (r\, c^2), \qquad d\Omega^2 = d\theta^2 + \sin^2\theta\, d\varphi^2$$

The definition has three properties. (i) Since $2n - 1 = 1 - 2GM/(rc^2) = 1 - r_s/r$, the metric is **identical** to the Schwarzschild geometry outside the event horizon; all the confirmed effects listed in Section 5.2 (GPS, light deflection, the perihelion shift of Mercury, the redshift of the star S2) are therefore recovered without any correction. This is the direct consequence of the network-level preservation of the equivalence principle discussed in Section 6.2: as the nodes compress, rulers and clocks, being made of the same nodes, compress with them; local physics is unchanged, only the comparison between different regions changes. (ii) The metric coefficient acquires a physical meaning: $2n - 1$ is twice the node compression minus one, and it vanishes at the event horizon. (iii) The metric yields natural markers in terms of n. The time dilation of a static body and of a body in circular orbit is

$$d\tau / dt = \sqrt{(2n - 1)} \qquad \text{(static body)} \qquad (12)$$

$$d\tau / dt = \sqrt{(3n - 2)} \qquad \text{(circular orbit, velocity effect included)} \qquad (13)$$

$$n = 1/2\text{: event horizon } (r = r_s); \qquad n = 2/3\text{: photon sphere } (r = 1.5\, r_s) \qquad (14)$$

$$n = 5/6\text{: ISCO } (r = 3\, r_s); \qquad n = 0\text{: core } (r = r_s/2 = GM/c^2)$$

Eq. (13) follows from the orbital velocity $v^2 = GM/r$ of a circular orbit, the total time dilation being $\sqrt{(1 - 3GM/(rc^2))}$; it vanishes at the photon sphere (n = 2/3), where light itself remains in circular orbit. For a general body $d\tau/dt = \sqrt{((2n - 1) - v_r^2/(c^2(2n - 1)) - r^2\Omega^2/c^2)}$. Fig. 8 shows the two functions and the markers, Fig. 9 the exterior geometry of the metric as a Flamm funnel coloured by node spacing, and Fig. 10 the time-dilation surface for a body in circular orbit; Table 3 compares values computed with the metric with observations.

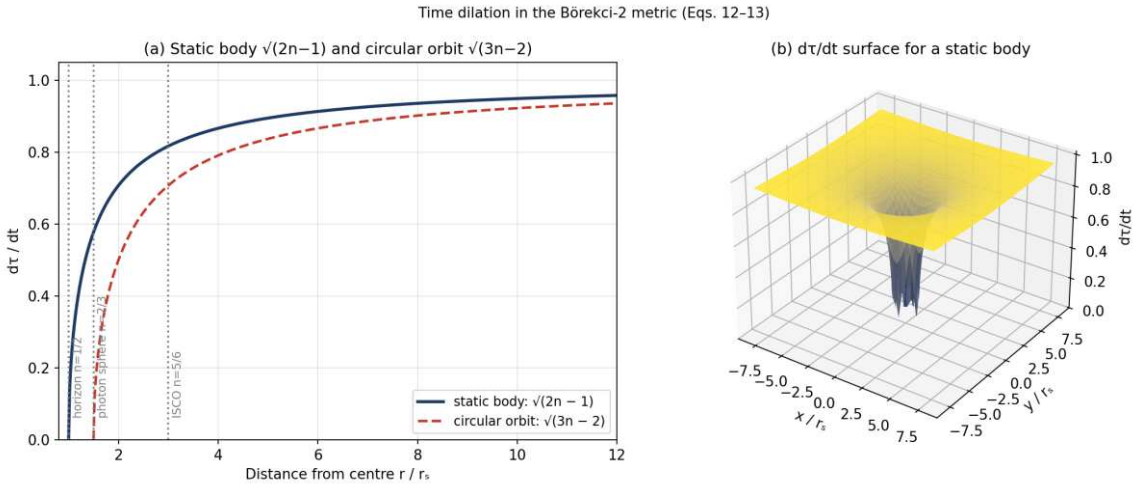


Fig. 8. Time dilation in the Börekci-2 metric. (a) $\sqrt{(2n-1)}$ for a static body and $\sqrt{(3n-2)}$ for a circular orbit; vertical lines mark the event horizon (n = 1/2), the photon sphere (n = 2/3) and the ISCO (n = 5/6). (b) Three-dimensional surface of dτ/dt for a static body around a black hole.

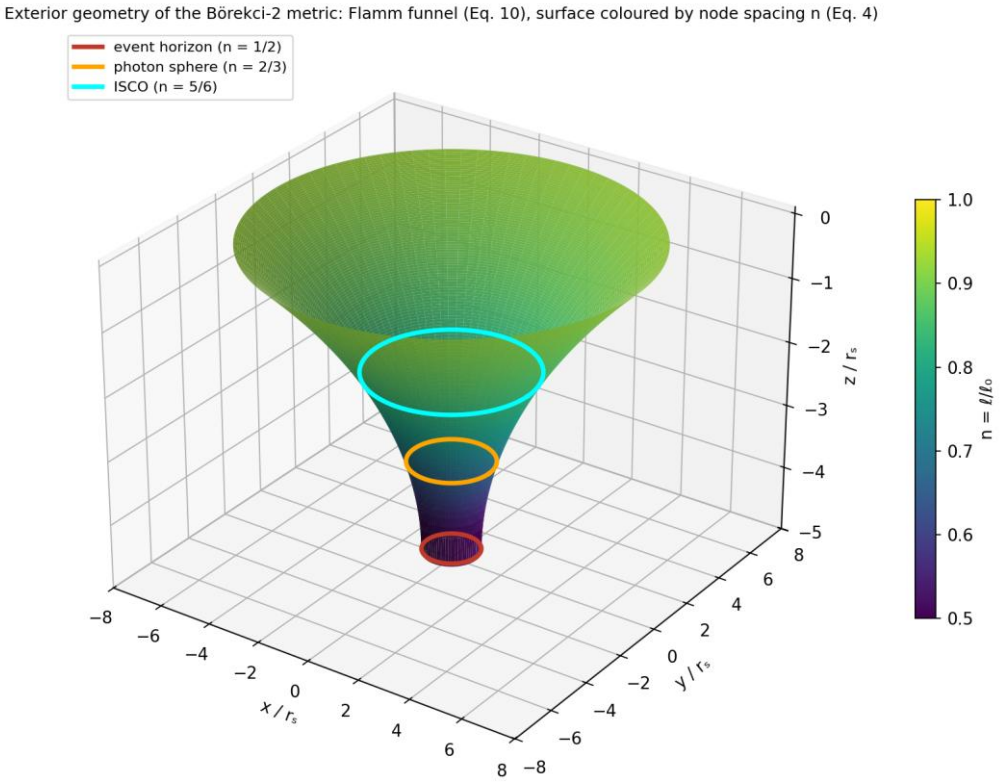



Fig. 9. Exterior geometry of the Börekci-2 metric: Flamm funnel (Eq. 10, in units of $r_s$), surface coloured by node spacing $n = \ell/\ell_0$ (Eq. 4). The rings mark the event horizon (n = 1/2), the photon sphere (n = 2/3) and the ISCO (n = 5/6); nodes compress toward the throat of the funnel.

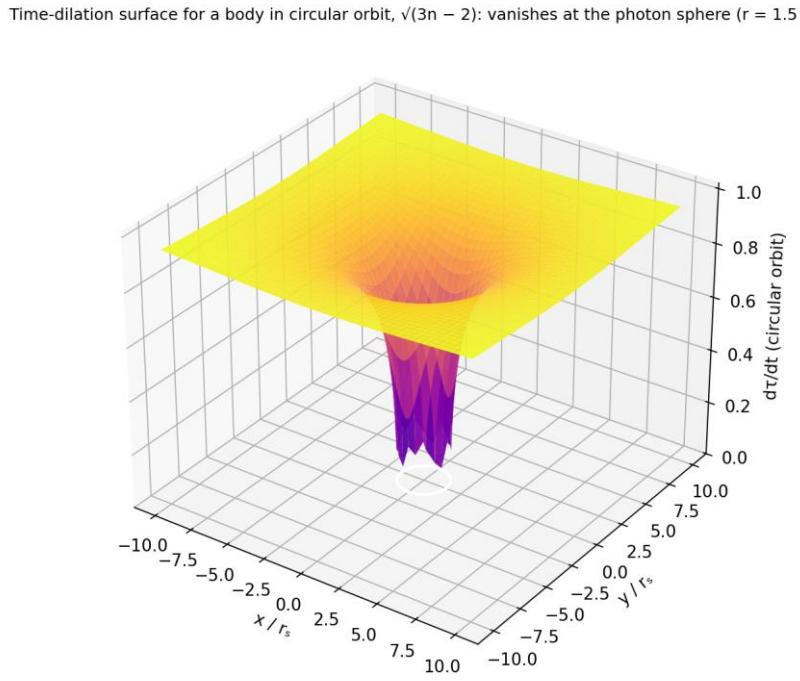


Fig. 10. Time-dilation surface for a body in circular orbit, $\sqrt{(3n - 2)}$ (Eq. 13). The surface vanishes at the photon sphere ($r = 1.5\ r_s$, $n = 2/3$); the dashed ring marks the ISCO ($r = 3\ r_s$).

**Table 3. Time dilations computed with the Börekci-2 metric and observations. Agreement is expected because the metric is identical to Schwarzschild outside; the table shows that the calculation in network language works.**

| Case | n − 1 | Börekci-2 metric calculation | Observation |
|---|---|---|---|
| Earth surface relative to a distant clock (Eq. 12) | $-6.96 \times 10^{-10}$ | 22 ms slow per year | consistent with redshift experiments [54] |
| GPS satellite relative to a ground clock (Eq. 13, r = 26 560 km) | $-1.67 \times 10^{-10}$ | +38.5 μs/day (gravity +45.7; velocity −7.2) | +38.6 μs/day [55] |
| Solar surface relative to a distant clock (Eq. 12) | $-2.12 \times 10^{-6}$ | 67 s slow per year | solar-line redshift [54] |
| Star S2 at pericentre of Sgr A* (r = 120 AU, v = 7650 km/s) | $-3.54 \times 10^{-4}$ | $z = 6.8 \times 10^{-4}$ (≈ 200 km/s equivalent) | ≈ 200 km/s [48] |

**Black-hole-matter surface and transition region.** In the linear form (Eq. 4) n vanishes at $r = GM/c^2 = r_s/2$; in the exact form (Eq. 4b) $n_e$ vanishes at the event horizon. According to the derivation of Section 5.1a the exact form is the valid one: the nodes touch at the horizon, the surface of black-hole matter coincides with the event horizon, and the network is not defined inside it. The model interprets this surface as the outer boundary of the black-hole matter that replaces the singularity (Section 4.1); the region $r_s/2 \le r \le r_s$ ($\Delta r/r_s = 1/2$) is the region over which the linear expansion spreads this surface inward, and it coincides with the upper end of the order-of-magnitude estimate of Section 6.3. For the surface to have an externally observable effect, its thickness and response must be derived from quantum dynamics (as in fuzzball and gravastar models); this is the only place where the metric could depart from Schwarzschild outside, and it is the open question of the paper. By Eq. (4c), Fig. 3b is both the $n_e$ surface and the time-dilation surface of the metric, while the linear n is the weak-field form of the network variable underlying the metric.

### *5.4 P3: gravity is set by the swallowed mass*

P3 is fully consistent with general relativity. Birkhoff's theorem [58] states that the spacetime outside a spherically symmetric mass distribution depends only on the total mass and is given, independently of the internal structure, by the Schwarzschild solution and hence by the Börekci-2 metric:

$$r_s = 2\,G\,M / c^2, \qquad dM / dt = F_{acc} - F_H \qquad (15)$$

where $F_{acc}$ is the mass–energy flux of infalling matter and radiation and $F_H$ the rate of mass loss through Hawking radiation, negligible for astrophysical black holes. The same relation resolves the apparent conflict between black-hole density and gravitational strength. The mean density inside the horizon is

$$\bar{\rho} = 3\,c^6 / (32\,\pi\,G^3\,M^2) \qquad (16)$$

**Table 4. Gravity strengthens with mass while mean density falls (water: 1000 kg/m³, air: 1.2 kg/m³).**

| Black hole | Mass | $r_s$ | Mean density $\bar{\rho}$ |
|---|---|---|---|
| Solar-mass | 1 $M_\odot$ | 2.95 km | $1.8 \times 10^{19}$ kg/m³ |
| Sgr A* (Milky Way centre) | $4.3 \times 10^6$ $M_\odot$ | $1.27 \times 10^{10}$ m (0.085 AU) | $1.0 \times 10^6$ kg/m³ |
| M87* | $6.5 \times 10^9$ $M_\odot$ | $1.92 \times 10^{13}$ m (128 AU) | 0.44 kg/m³ |

As a black hole swallows matter its mass and gravity grow while its mean density falls with the square of the mass (Table 4). Gravity is set by the swallowed mass, not by density; in the model the decisive quantity is the node compression at the horizon (n = 1/2), the same for every black hole.

### *5.5 P4: everything swallowed becomes black-hole matter*

Whatever falls into a black hole, its contribution to the mass is set only by the total energy it carries:

$$\Delta M = \Delta E_{acc} / c^2 \qquad (17)$$

Following Wheeler's conjecture, Bekenstein [59] showed that no baryon number can be assigned to a static black hole by external measurements; baryon-number conservation is transcended in black-hole physics. The Hawking temperature depends on mass alone:

$$T_H = \hbar c^3 / (8 \pi G M k_B) \qquad (18)$$

The particles emitted by an evaporating black hole do not, to first approximation, carry the identity of the matter that fell in [26, 60]. This is the strongest support for P4 in the literature. On the other hand, the entropy of a black hole is proportional to the area of its horizon [61]:

$$S_{BH} = k_B A / (4 \ell_P^2), \qquad A = 4 \pi r_s^2 \qquad (19)$$

For a solar-mass black hole $S_{BH} \approx 1.0 \times 10^{77}$ $k_B$, whereas the same mass contains about $1.2 \times 10^{57}$ protons. The black hole is the highest-entropy state this mass can reach and has of order $\exp(10^{77})$ internal states [62]. Recent work on the information problem indicates that information falling into a black hole is not destroyed [63, 64, 65].

> **Adopted form of P4.** Black-hole matter is a single kind of matter that can occupy a very large number of internal states. In the water analogy: all water molecules are identical, yet their arrangement can carry information. This form is consistent with both the no-hair theorem and information preservation.

### *5.6 Scope decisions*

- **Accelerated expansion is outside the scope.** In the model the fabric is net attractive and cannot explain the accelerated expansion discovered in 1998 [66, 67]; the dark-energy density is about $6 \times 10^{-27}$ kg/m³ and stays constant as space expands [68], whereas a dilute matter would dilute with volume.

- **The dark-matter claim is outside the scope.** The idea that dark matter could be an intermediate-density state of the fabric requires quantitative support and is not treated here.

## 6. Predictions and current experimental constraints

### *6.1 Dispersion of gravitational waves: unmeasurable*

In a network-structured spacetime the wave speed may depend on frequency as the wavelength approaches the node spacing:

$$\Delta v / c \sim (\ell_P / \lambda)^n, \quad n = 1 \text{ or } 2 \qquad (20)$$

In the LIGO band ($f = 100$ Hz, $\lambda \approx 3\,000$ km) this ratio is $5.4 \times 10^{-42}$ for $n = 1$ and $2.9 \times 10^{-83}$ for $n = 2$; the limit set by GW170817 is $\sim 10^{-15}$ [69]. The prediction lies 27–68 orders of magnitude below the measurement limit.

### *6.2 Local position invariance and the network-level preservation of the equivalence principle*

The hypothesis interprets virtual-quark production as an activity of the black-hole matter constituting spacetime and states that the compression of this matter depends on the gravitational potential. Unless the two statements are separated carefully, a measurable consequence follows. The dependence of a local constant on the potential is parametrised by a standard coefficient:

$$\delta\varepsilon / \varepsilon = k_\varepsilon \cdot \Delta\Phi / c^2 \qquad (21)$$

**Naive reading.** If the QCD scale is taken inversely proportional to the node spacing, Eq. (4) gives

$$\delta m_p / m_p \approx -\delta\ell / \ell = |\Phi| / c^2 \quad \Longrightarrow \quad k_\mu \approx 1 \qquad (22)$$

This reading has been measured directly and is excluded. Along the Earth's orbit the solar potential oscillates by about $3 \times 10^{-10}$ per year (the variation of the value in Table 2 due to the orbital eccentricity). Lange et al. [70], comparing ytterbium-ion optical clocks with caesium fountain clocks over several years, obtained $(c^2/\mu)(d\mu/d\Phi) = 7(45) \times 10^{-8}$, $(c^2/\alpha)(d\alpha/d\Phi) = 14(11) \times 10^{-9}$ and $(c^2/X_q)(dX_q/d\Phi) = -21(23) \times 10^{-7}$ ($X_q = m_q/\Lambda_{QCD}$); Guéna et al. [71] had earlier reported similar limits. The prediction of the naive reading lies about six orders of magnitude above these limits (Fig. 11).

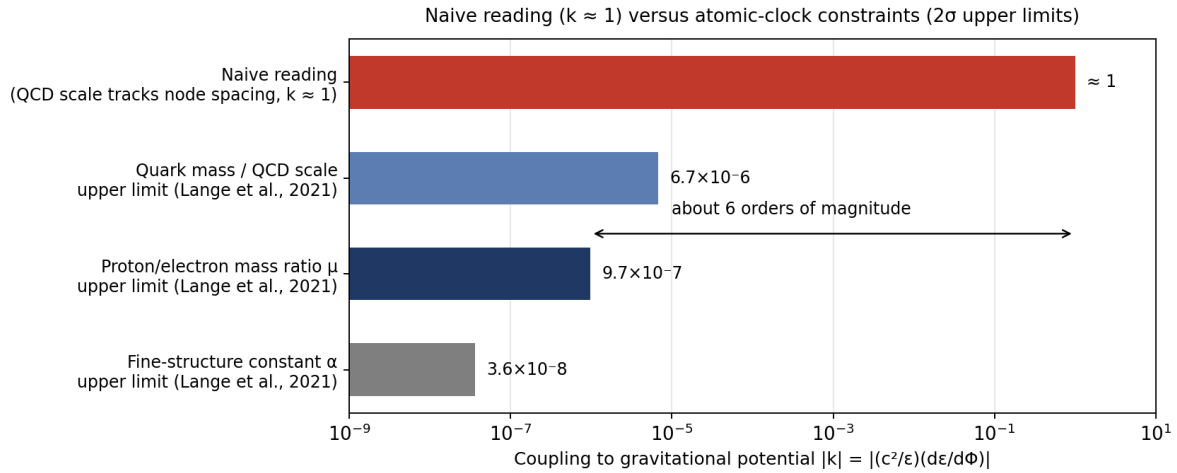



Fig. 11. The naive reading (k ≈ 1) versus the 2σ upper limits from atomic-clock measurements. The naive reading is excluded by six orders of magnitude; the network-level equivalence reading (below) gives k = 0 and is consistent with these limits.

**Network-level equivalence reading.** The naive reading overlooks one thing: as the nodes compress, not only "empty space" compresses. Atoms, rulers, clocks and the proton itself are made of the same nodes and compress together. A local measurement is always a ratio of two local quantities; when numerator and denominator change by the same factor the ratio does not change. Local constants such as the QCD scale, the proton mass and the fine-structure constant therefore remain independent of the potential: $k_\varepsilon = 0$. The effect of node compression appears only when clocks or rulers at **two different potentials** are compared; that comparison is the subject of the Börekci-2 metric (Eqs. 11–13) and of Table 3, and it is the observed gravitational redshift itself. The shortening of Eq. (4) is thus the network-language counterpart of the metric coefficient of general relativity; the equivalence principle is preserved at the network level.

> **Conclusion.** The model is consistent with local-position-invariance measurements, and this consistency is not a tuning but a structural consequence of the network. The price is explicit: in the weak field the model is indistinguishable from general relativity; the distinguishing prediction is the transition region at the event horizon (Section 6.3). Loop quantum gravity is in the same position. Whether a small deviation remains is an experimental question: if k is left free, the current limit is $|k_\mu| < 10^{-6}$ and the next generation of optical clocks will push it to the $10^{-8}$ level; for the model to predict a non-zero k at that level a derivation is required, which is not provided in this paper.

### *6.3 A transition region at the event horizon: testable*

The model predicts that the event horizon lies at the radius predicted by Einstein but is a transition region of finite thickness rather than a sharp surface. According to Section 5.1a the black-hole-matter surface lies at the event horizon; the linear expansion spreads it over a region of thickness $\Delta r/r_s = 1/2$. For an externally observable effect this structure must modify the horizon, at a level of order

$$\Delta r / r_s \sim 0.1 - 0.5 \qquad (23)$$

A thick transition region blurs the edge of the black-hole shadow and changes the ring width; the M87* and Sgr A* shadows agree with general relativity at the ~10–17% level [50, 51]. Gravitational-wave observations search for echoes from a structure near the horizon; no confirmed signal exists. The upper part of the range in Eq. (23) may already be constrained by existing data; the magnitude of the external effect must be derived from the core dynamics.

### *6.4 Observational difference from the vecro hypothesis: a stiff-fluid era in the early universe*

In Section 3.2 the difference between the vecro hypothesis and the present one was the interpretation of empty space as a real state of matter rather than as virtual fluctuations. This difference has an observational consequence. In Mathur's model the vecros are stretched in an expanding universe and generate vacuum energy; the equation of state of empty space is that of dark energy ($w = p/\rho c^2 = -1$). In the present hypothesis black-hole matter is net attractive (Section 5.6), and its densest state at the beginning of the universe is a stiff fluid, like the black-hole gas of Banks and Fischler [42] and the vecro gas of Brandenberger and Mitchell [38]: $p = \rho c^2$, $w = 1$. The two hypotheses thus sit at opposite extremes of the equation of state of empty space, and this leaves a trace in the expansion history of the early universe.

The primordial gravitational-wave spectrum emerging from inflation is flat during radiation domination, but acquires a blue tilt for modes entering the horizon while the universe expands with an equation of state stiffer than radiation ($w > 1/3$) [72, 73, 74]:

$$n_T = d \ln \Omega_{GW} / d \ln f = 2 (w - 1/3) / (w + 1/3) \quad \Longrightarrow \quad w = 1: \ \Omega_{GW} \propto f \qquad (24)$$

The hypothesis therefore predicts that the primordial gravitational-wave background rises as $\Omega_{GW} \propto f$ above the frequency $f_{RD}$ corresponding to the stiff-to-radiation transition (Fig. 12). The vecro interpretation requires no such era. The prediction is testable with LIGO/Virgo, LISA and the Einstein Telescope; the duration of the stiff era is bounded by the big-bang-nucleosynthesis limit on the gravitational-wave energy density [74]. Because the end temperature of the stiff era is not yet fixed within the hypothesis, $f_{RD}$ is a free parameter; the measurable prediction of the hypothesis is the sign and magnitude of the tilt ($n_T = 1$), not its location.

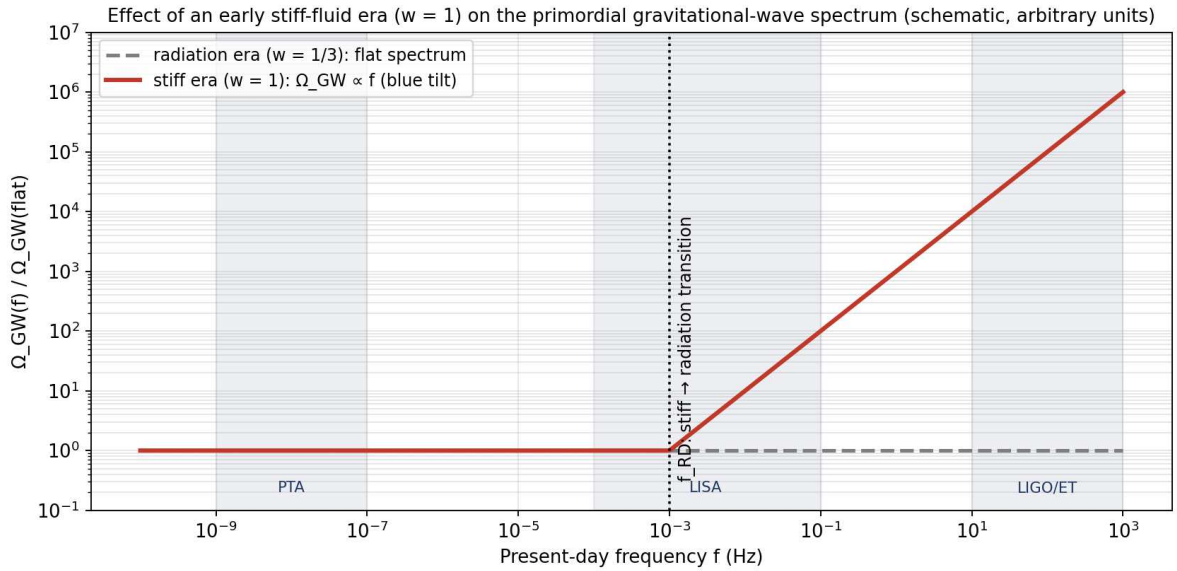



Fig. 12. Effect of an early stiff-fluid era (w = 1) on the primordial gravitational-wave spectrum (schematic, arbitrary units). The spectrum is flat in the radiation era; for modes entering the horizon during the stiff era, $\Omega_{GW} \propto f$ (Eq. 24). The transition frequency $f_{RD}$ is free within the hypothesis; the shaded bands indicate the sensitivity ranges of PTA, LISA and LIGO/Einstein Telescope.

## 7. Discussion

**Table 5. Counterparts of the propositions in the literature and their original aspects.**

| Proposition | Counterpart in the literature | Original aspect of the hypothesis |
|---|---|---|
| P1 | The vacuum is structured and energetic (Section 2); spacetime may be emergent (3.1); the vecro hypothesis proposes virtual black-hole microstates in the vacuum (3.2). | Empty space as a real, dilute state of black-hole matter rather than virtual fluctuations; this matter as the ancestor of all elements (3.3, 4.3). |
| P2 | Node–link structure: spin networks, quantum graphity (3.1). | Nodes made of black-hole matter; spacing shortening with potential (Eq. 4), its derivation from the constant-proper-spacing postulate (5.1a) and the Börekci-2 metric (5.3). |
| P3 | Birkhoff's theorem (5.4). | Identical to general relativity; a consistency condition. |
| P4 | Mass–energy equivalence; unmeasurability of baryon number; Hawking temperature; Bekenstein–Hawking entropy (5.5). | Conversion of swallowed matter into a single substance that stores information in its internal states. |

The findings of Section 2 show conclusively that the quantum vacuum is not empty; they are, however, explained quantitatively by quantum field theory and QCD without recourse to black-hole matter. They are therefore consistent with the hypothesis but do not prove it. The closest theoretical work is the vecro hypothesis; the difference is the interpretation of empty space as a real state of matter rather than virtual fluctuations. The Börekci-2 metric shows how this interpretation can be constructed without conflicting with general relativity, but for the same reason it yields no new weak-field prediction; the observational consequence of the difference

lies in the equation of state of the early universe (Section 6.4). For a peer-reviewed defence the following steps are required:

1. The thickness of the black-hole-matter surface at the horizon and its effect on the exterior geometry must be derived from the network dynamics and compared with published EHT and ringdown constraints.
2. Eq. (4b) has been derived from the constant-proper-spacing postulate (Section 5.1a), but the Einstein equations remain an input. The metric must be obtained dynamically from a link-energy principle.
3. The end temperature of the stiff era, and hence $f_{RD}$ of Section 6.4, must be fixed from within the hypothesis.
4. A property must be defined that distinguishes black-hole matter from the quark–gluon plasma and from the QCD vacuum.
5. The vacuum energy naively predicted by quantum field theory exceeds the observed dark-energy density by about $10^{120}$ [75]; any hypothesis interpreting the vacuum as a state of matter must confront this discrepancy.
6. The collapse-halting mechanism (Section 4.1) must be justified within the hypothesis's own framework.
7. If a small deviation from the network-level equivalence principle is to be predicted (Section 6.2), the coefficient k must be derived.

## 8. Conclusions

Strong experimental evidence shows that the quantum vacuum is not empty, that it has a rich structure including virtual quark pairs, and that this structure can turn into real particles; the 2026 STAR result is the most recent example at the quark level. The idea that spacetime emerges from a more fundamental structure, and the relation of black holes to the origin of the universe, have a well-established theoretical literature. This hypothesis, Börekci's Hypothesis of Black-Hole Matter as the Primary Substance of the Universe, defines spacetime geometry as a structure made of black-hole matter joined by special links, mobile and changing according to the gravity and energy within it, and proposes this matter as the common ancestor of all matter, energy and geometry. The calculations around the Sun, Earth and Moon show that "curvature" in the hypothesis must be understood as depth. The node-spacing relation derived from the constant-proper-spacing postulate, and the Börekci-2 metric defined from it, are identical to the Schwarzschild geometry outside the horizon; they reproduce observations such as GPS and the star S2 in network language, yield natural markers for the event horizon, the photon sphere and the ISCO, and place the black-hole-matter surface at the event horizon. Because node compression affects all local scales together, the equivalence principle is preserved at the network level; the model is consistent with atomic-clock constraints but, for the same reason, indistinguishable from general relativity in the weak field. P3 is consistent

with general relativity; P4 is supported by three well-known results of black-hole physics. P1 and P2 are original propositions; two routes make them testable: deriving the effect of the black-hole-matter surface at the horizon on the exterior geometry, and searching for the blue tilt that an early stiff-fluid era imprints on the primordial gravitational-wave spectrum.

## Declarations

**Funding.** Dr. Hasan Börekci received no institutional support for the design or writing of this work; he is not employed by any state-affiliated institution and wrote it with his own means.

**Author contribution.** The conception, planning and apparatus design are the author's own.

**Use of artificial intelligence.** Artificial intelligence was used for the literature search, calculations and page layout; responsibility for the scientific content and conclusions rests with the author.

**Competing interests.** The author declares no competing interests.

**Data availability.** All numerical values in the paper can be reproduced from the equations given in the text and the published constants in the cited references. No new datasets were generated.

**Ethics approval and consent to participate.** Not applicable.

**Consent for publication.** Not applicable.

**Acknowledgements.** None.

## References

[1] Riek, C., Seletskiy, D. V., Moskalenko, A. S., Schmidt, J. F., Krauspe, P., Eckart, S., Eggert, S., Burkard, G., Leitenstorfer, A.: Direct sampling of electric-field vacuum fluctuations. Science 350, 420–423 (2015)

[2] STAR Collaboration: Measuring spin correlation between quarks during QCD confinement. Nature 650, 65–71 (2026). https://doi.org/10.1038/s41586-025-09920-0

[3] Israel, W.: Event horizons in static vacuum space-times. Phys. Rev. 164, 1776–1779 (1967)

[4] Casimir, H.B.G.: On the attraction between two perfectly conducting plates. Proc. K. Ned. Akad. Wet. 51, 793–795 (1948)

[5] Lamoreaux, S.K.: Demonstration of the Casimir force in the 0.6 to 6 μm range. Phys. Rev. Lett. 78, 5–8 (1997)

[6] Bressi, G., Carugno, G., Onofrio, R., Ruoso, G.: Measurement of the Casimir force between parallel metallic surfaces. Phys. Rev. Lett. 88, 041804 (2002)

[7] Lamb, W.E., Retherford, R.C.: Fine structure of the hydrogen atom by a microwave method. Phys. Rev. 72, 241–243 (1947)

[8] Bethe, H.A.: The electromagnetic shift of energy levels. Phys. Rev. 72, 339–341 (1947)

[9] Benea-Chelmus, I.-C., Settembrini, F.F., Scalari, G., Faist, J.: Electric field correlation measurements on the electromagnetic vacuum state. Nature 568, 202–206 (2019)

[10] Wilson, C.M., Johansson, G., Pourkabirian, A., Simoen, M., Johansson, J.R., Duty, T., Nori, F., Delsing, P.: Observation of the dynamical Casimir effect in a superconducting circuit. Nature 479, 376–379 (2011)

[11] Schwinger, J.: On gauge invariance and vacuum polarization. Phys. Rev. 82, 664–679 (1951)

[12] STAR Collaboration: Measurement of $e^+e^-$ momentum and angular distributions from linearly polarized photon collisions. Phys. Rev. Lett. 127, 052302 (2021)

[13] ATLAS Collaboration: Evidence for light-by-light scattering in heavy-ion collisions with the ATLAS detector at the LHC. Nat. Phys. 13, 852–858 (2017)

[14] Shifman, M.A., Vainshtein, A.I., Zakharov, V.I.: QCD and resonance physics. Theoretical foundations. Nucl. Phys. B 147, 385–447 (1979)

[15] Dürr, S., et al.: Ab initio determination of light hadron masses. Science 322, 1224–1227 (2008)

[16] Dove, J., et al. (SeaQuest Collaboration): The asymmetry of antimatter in the proton. Nature 590, 561–565 (2021)

[17] Sakharov, A.D.: Vacuum quantum fluctuations in curved space and the theory of gravitation. Dokl. Akad. Nauk SSSR 177, 70–71 (1967) [Sov. Phys. Dokl. 12, 1040 (1968)]

[18] Jacobson, T.: Thermodynamics of spacetime: the Einstein equation of state. Phys. Rev. Lett. 75, 1260–1263 (1995)

[19] Volovik, G.E.: The Universe in a Helium Droplet. Oxford University Press, Oxford (2003)

[20] Barceló, C., Liberati, S., Visser, M.: Analogue gravity. Living Rev. Relativ. 14, 3 (2011)

[21] Rovelli, C., Smolin, L.: Spin networks and quantum gravity. Phys. Rev. D 52, 5743–5759 (1995)

[22] Konopka, T., Markopoulou, F., Severini, S.: Quantum graphity: a model of emergent locality. Phys. Rev. D 77, 104029 (2008)

[23] Van Raamsdonk, M.: Building up spacetime with quantum entanglement. Gen. Relativ. Gravit. 42, 2323–2329 (2010)

[24] Verlinde, E.: On the origin of gravity and the laws of Newton. J. High Energy Phys. 2011(4), 029 (2011)

[25] Hawking, S.W.: Black hole explosions? Nature 248, 30–31 (1974)

[26] Hawking, S.W.: Particle creation by black holes. Commun. Math. Phys. 43, 199–220 (1975)

[27] Muñoz de Nova, J.R., Golubkov, K., Kolobov, V.I., Steinhauer, J.: Observation of thermal Hawking radiation and its temperature in an analogue black hole. Nature 569, 688–691 (2019)

[28] Mazur, P.O., Mottola, E.: Gravitational vacuum condensate stars. Proc. Natl. Acad. Sci. USA 101, 9545–9550 (2004)

[29] Mathur, S.D.: The fuzzball proposal for black holes: an elementary review. Fortschr. Phys. 53, 793–827 (2005)

[30] Rovelli, C., Vidotto, F.: Planck stars. Int. J. Mod. Phys. D 23, 1442026 (2014)

[31] Wheeler, J.A.: On the nature of quantum geometrodynamics. Ann. Phys. 2, 604–614 (1957)

[32] Hawking, S.W.: Virtual black holes. Phys. Rev. D 53, 3099–3107 (1996)

[33] Mäkelä, J.: Vacuum energy, black holes and the cosmological constant. Essay, Gravity Research Foundation 2014 Awards. arXiv:1402.1488 (2014)

[34] Mathur, S.D.: The vecro hypothesis. Int. J. Mod. Phys. D 29(15), 2030009 (2020)

[35] Mathur, S.D.: The elastic vacuum. Essay, Gravity Research Foundation 2021 Awards (2021)

[36] Mathur, S.D.: The secret structure of the gravitational vacuum. Essay, Gravity Research Foundation 2024 Awards. arXiv:2405.08945 (2024)

[37] Mathur, S.D.: The magic of the gravitational vacuum. arXiv:2606.20334 (2026)

[38] Brandenberger, R., Mitchell, G.A.: A bouncing cosmology from VECROs. Eur. Phys. J. C 83 (2023). https://doi.org/10.1140/epjc/s10052-023-11501-2

[39] Pathria, R.K.: The universe as a black hole. Nature 240, 298–299 (1972)

[40] Smolin, L.: Did the universe evolve? Class. Quantum Grav. 9, 173–191 (1992)

[41] Popławski, N.J.: Radial motion into an Einstein–Rosen bridge. Phys. Lett. B 687, 110–113 (2010)

[42] Banks, T., Fischler, W.: An holographic cosmology. arXiv:hep-th/0111142 (2001)

[43] Hawking, S.W.: Gravitationally collapsed objects of very low mass. Mon. Not. R. Astron. Soc. 152, 75–78 (1971)

[44] ’t Hooft, G.: The black hole interpretation of string theory. Nucl. Phys. B 335, 138–154 (1990)

[45] Holzhey, C.F.E., Wilczek, F.: Black holes as elementary particles. Nucl. Phys. B 380, 447–477 (1992)

[46] Horowitz, G.T., Polchinski, J.: A correspondence principle for black holes and strings. Phys. Rev. D 55, 6189–6197 (1997)

[47] Dvali, G., Gomez, C.: Black hole's quantum N-portrait. Fortschr. Phys. 61, 742–767 (2013)

[48] GRAVITY Collaboration: Detection of the gravitational redshift in the orbit of the star S2 near the Galactic centre massive black hole. Astron. Astrophys. 615, L15 (2018)

[49] GRAVITY Collaboration: Detection of the Schwarzschild precession in the orbit of the star S2 near the Galactic centre massive black hole. Astron. Astrophys. 636, L5 (2020)

[50] Event Horizon Telescope Collaboration: First M87 Event Horizon Telescope results. I. The shadow of the supermassive black hole. Astrophys. J. Lett. 875, L1 (2019)

[51] Event Horizon Telescope Collaboration: First Sagittarius A* Event Horizon Telescope results. I. The shadow of the supermassive black hole in the center of the Milky Way. Astrophys. J. Lett. 930, L12 (2022)

[52] Abbott, B.P., et al. (LIGO Scientific Collaboration and Virgo Collaboration): Tests of general relativity with GW150914. Phys. Rev. Lett. 116, 221101 (2016)

[53] Penrose, R.: Gravitational collapse and space-time singularities. Phys. Rev. Lett. 14, 57–59 (1965)

[54] Will, C.M.: The confrontation between general relativity and experiment. Living Rev. Relativ. 17, 4 (2014)

[55] Ashby, N.: Relativity in the Global Positioning System. Living Rev. Relativ. 6, 1 (2003)

[56] Dyson, F.W., Eddington, A.S., Davidson, C.: A determination of the deflection of light by the Sun's gravitational field, from observations made at the total eclipse of May 29, 1919. Phil. Trans. R. Soc. A 220, 291–333 (1920)

[57] Flamm, L.: Beiträge zur Einsteinschen Gravitationstheorie. Phys. Z. 17, 448–454 (1916)

[58] Birkhoff, G.D.: Relativity and Modern Physics. Harvard University Press, Cambridge, MA (1923)

[59] Bekenstein, J.D.: Nonexistence of baryon number for static black holes. Phys. Rev. D 5, 1239–1246 (1972)

[60] Hawking, S.W.: Breakdown of predictability in gravitational collapse. Phys. Rev. D 14, 2460–2473 (1976)

[61] Bekenstein, J.D.: Black holes and entropy. Phys. Rev. D 7, 2333–2346 (1973)

[62] Strominger, A., Vafa, C.: Microscopic origin of the Bekenstein–Hawking entropy. Phys. Lett. B 379, 99–104 (1996)

[63] Page, D.N.: Information in black hole radiation. Phys. Rev. Lett. 71, 3743–3746 (1993)

[64] Almheiri, A., Engelhardt, N., Marolf, D., Maxfield, H.: The entropy of bulk quantum fields and the entanglement wedge of an evaporating black hole. J. High Energy Phys. 2019(12), 063 (2019)

[65] Penington, G.: Entanglement wedge reconstruction and the information paradox. J. High Energy Phys. 2020(9), 002 (2020)

[66] Riess, A.G., et al.: Observational evidence from supernovae for an accelerating universe and a cosmological constant. Astron. J. 116, 1009–1038 (1998)

[67] Perlmutter, S., et al.: Measurements of $\Omega$ and $\Lambda$ from 42 high-redshift supernovae. Astrophys. J. 517, 565–586 (1999)

[68] Planck Collaboration: Planck 2018 results. VI. Cosmological parameters. Astron. Astrophys. 641, A6 (2020)

[69] Abbott, B.P., et al.: Gravitational waves and gamma-rays from a binary neutron star merger: GW170817 and GRB 170817A. Astrophys. J. Lett. 848, L13 (2017)

[70] Lange, R., Huntemann, N., Rahm, J.M., Sanner, C., Shao, H., Lipphardt, B., Tamm, Chr., Weyers, S., Peik, E.: Improved limits for violations of local position invariance from atomic clock comparisons. Phys. Rev. Lett. 126, 011102 (2021)

[71] Guéna, J., Abgrall, M., Rovera, D., Rosenbusch, P., Tobar, M.E., Laurent, Ph., Clairon, A., Bize, S.: Improved tests of local position invariance using $^{87}$Rb and $^{133}$Cs fountains. Phys. Rev. Lett. 109, 080801 (2012)

[72] Giovannini, M.: Gravitational waves constraints on post-inflationary phases stiffer than radiation. Phys. Rev. D 58, 083504 (1998)

[73] Sahni, V., Sami, M., Souradeep, T.: Relic gravity waves from braneworld inflation. Phys. Rev. D 65, 023518 (2002)

[74] Figueroa, D.G., Tanin, E.H.: Ability of LIGO and LISA to probe the equation of state of the early Universe. J. Cosmol. Astropart. Phys. 2019(08), 011 (2019)

[75] Weinberg, S.: The cosmological constant problem. Rev. Mod. Phys. 61, 1–23 (1989)